

MDPI

Article

Growth of Highly Transparent Amorphous Carbon Films Using Beam Plasma Source

Youngsuk Kim ¹, Nina Baule ², Maheshwar Shrestha ³ and Qi Hua Fan ^{1,4,*}

- Department of Chemical Engineering and Materials Science, Michigan State University, East Lansing, MI 48824, USA
- ² Fraunhofer USA Center Midwest, East Lansing, MI 48824, USA
- Scion Plasma LLC, East Lansing, MI 48823, USA
- Department of Electrical and Computer Engineering, Michigan State University, East Lansing, MI 48824, USA
- * Correspondence: qfan@egr.msu.edu

Abstract: A single beam plasma source was used to deposit hydrogenated amorphous carbon (a-C:H) coatings at room temperature. Using methane source gas, a-C:H coatings were deposited at different radio frequency (RF) power to fabricate transparent and durable coatings. The film deposition rate was almost linearly proportional to the ion source power. Hydrogenated amorphous carbon films of ~100 nm thickness appeared to be highly transparent from UV to the infrared range with a transmittance of ~90% and optical bandgap of ~3.7 eV. The coatings also possess desirable mechanical properties with Young's modulus of ~78 GPa and density of ~1.9 g/cm³. The combined material properties of high transmittance and high durability make the ion-source-deposited a-C:H coatings attractive for many applications.

Keywords: transparent carbon film; ion source; plasma-enhanced chemical vapor deposition



Citation: Kim, Y.; Baule, N.; Shrestha, M.; Fan, Q.H. Growth of Highly Transparent Amorphous Carbon Films Using Beam Plasma Source. *Coatings* **2022**, *12*, 1159. https://doi.org/10.3390/ coatings12081159

Academic Editor: Ross Birney

Received: 6 July 2022 Accepted: 6 August 2022 Published: 11 August 2022

Publisher's Note: MDPI stays neutral with regard to jurisdictional claims in published maps and institutional affiliations.



Copyright: © 2022 by the authors. Licensee MDPI, Basel, Switzerland. This article is an open access article distributed under the terms and conditions of the Creative Commons Attribution (CC BY) license (https://creativecommons.org/licenses/by/4.0/).

1. Introduction

Amorphous carbon (a-C) coatings have many attractive properties, such as high hardness, low friction, low roughness, and high resistivity [1–3]. By adding hydrogen to form hydrogenated amorphous carbon (a-C:H), the coatings become softer but more transparent than a-C [4]. Therefore, a-C:H is particularly suitable for applications where highly transparent and moderate wear-resistant coatings are required. Examples of applications include moisture barrier and wear-resistant coatings for perovskite solar cells, plastic packaging materials, and touch screens.

Hydrogenated amorphous carbon coatings have been produced by physical vapor deposition (PVD), chemical vapor deposition (CVD), and plasma-enhanced chemical vapor deposition (PECVD) [1,4,5]. Today, PECVD is the most used method for making a-C:H coatings because of its ability to tune the process and, subsequently, the material structure and properties [6–8].

Most of the past studies aimed to achieve a specific property of amorphous carbon coatings, such as high hardness [9,10]. A few reports discussed the growth of a-C:H coatings that had combined high transmittance and mechanical strength (e.g., Young's modulus and hardness) [11–17]. Producing highly transparent a-C:H with high density and hardness is a challenge to conventional PECVD [9,17–19]. The limitation arises from the plasma characteristic of PECVD, in which the chemical species are not under thermal equilibrium [20]. This means the average electron energy (e.g., 3 eV) is much higher than the ions (e.g., ~0.07 eV) and the neutral species (e.g., ~0.03 eV). Therefore, the ions and neutral species have little kinetic energy as they reach the substrate. It has been demonstrated that applying a negative bias to the substrate can effectively densify the a-C:H by attracting the positively charged ions to bombard the growing film [21]. Although applying a negative bias could be difficult in some applications, such as coatings on a

Coatings **2022**, 12, 1159 2 of 7

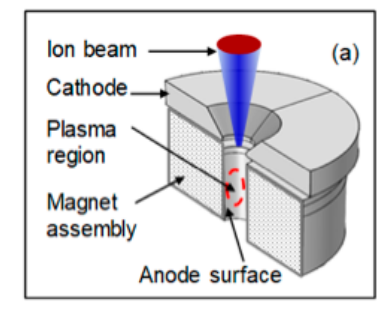
plastic sheet in a continuous roll-to-roll process, this idea has inspired the use of ion source to deposit transparent a-C:H coatings with high Young's modulus.

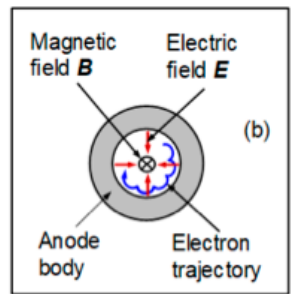
Ion sources are plasma generation devices that enable ion beams to interact with the materials at the atomic level as they are deposited to effectively modulate the film microstructure [21-25]. In the ion-source-enhanced growth of a-C:H, the ion source produces plasma from hydrocarbon gas, such as methane. The plasma breaks the hydrocarbon molecules and creates various radicals that form amorphous carbon coatings. Since the pioneering work of Aisenberg and Chabot [26], ion beam deposition of amorphous carbon thin films has continuously advanced with the development of ion sources. Two major types of ion sources have been widely used for thin-film processing, gridded and end-Hall ion sources [27,28]. The gridded ion source has a relatively low current and high ion energy (e.g., >300 eV), which usually leads to large stress and graphitization of the carbon films. Gridless end-Hall ion sources can produce ions with a wide range of average energy (e.g., 40–200 eV) at a much higher current than gridded ion sources. These characteristics are beneficial for the high-rate deposition of dense a-C:H films. The requirement for a closed-loop drift of the electrons in end-Hall ion sources leads to circular or racetrack beam patterns, while some applications would demand the ions to be focused onto a specific area. Furthermore, end-Hall ion sources have a narrow ion-emitting slit, which could be coated quickly, resulting in unstable discharges.

This work reports the use of a recently developed single beam plasma source to address the needs described above. The goal is to demonstrate the feasibility of low-temperature growth of highly transparent and dense a-C:H films with moderate Young's modulus.

2. Material and Method

The depositions were performed in a custom-made vacuum system with a load lock. A single beam ion source (SPR-10, Scion Plasma LLC) illustrated in Figure 1a,b was used as the plasma source. It consists of an anode with a center cavity and a closed bottom. The anode opening is 12 mm in diameter. A cathode cover is located above the anode. A magnet assembly generates a magnetic field that forms a closed loop inside the anode cavity to confine the electrons. Details of this single beam plasma source can be found in reference [29]. The distance from the substrate to the ion source was set at 38 mm, which is shown in Figure 1c.





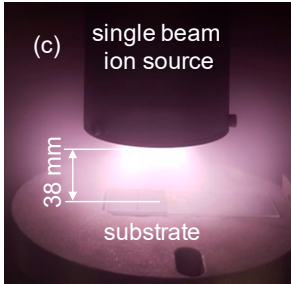


Figure 1. (a) Profile side view and (b) top view of the single beam plasma source. (c) Plasma discharge image of the single beam ion source.

The process gases were methane (CH₄, 10%) mixed with argon (Ar, 90%). The base pressure for the deposition was $<8\times10^{-4}$ Pa. The deposition pressure was 1.6 Pa. The deposition was performed on 25×25 mm² glass and Si wafer substrates at room temperature. The substrates were ultrasonically cleaned in acetone and methanol in sequence, each for 15 min. Then the substrates were dried using compressed nitrogen gas and placed in an oven at 80 °C for 30 min.

The ion source was excited by a radio frequency (RF) power of 13.56 MHz. The RF power used was in the range of 10 to 40 W. At different RF excitation power, the deposition time was adjusted to make the coatings of 100 nm thickness.

Coatings 2022, 12, 1159 3 of 7

The thickness of the coatings was measured by a Dektak XT profilometer system. The thickness was measured three times and averaged.

To determine the chemical composition of the a-C:H films, X-ray photoelectron spectroscopy (XPS; Perkin Elmer Phi 5400 ESCA system) with non-monochromatic aluminum $K\alpha$ X-ray source was employed. Carbon (C1s) was used to calibrate the sample charging for XPS measurements. The XPS data were fit using the PHI Multipak (v8.0) software.

A laser acoustic surface wave spectroscopy instrument (LAwave) was used to measure the elastic properties and density of the coatings.

The optical transmittance of the coatings was measured by a spectrophotometer (F20, Filmetrics) and a clean glass slide was used as a baseline for comparison.

The surface morphology was measured by atomic force microscopy (AFM Hitachi AFM 5100N) with a Si tip and the aerial root mean square roughness (S_q) was calculated.

3. Results and Discussion

The a-C:H coatings were deposited at different RF power. Figure 2a shows the film deposition rate dependence on the power. The deposition rates were deduced from the film thicknesses and deposition times. It can be seen that the deposition rates increased with the RF power because a higher RF power resulted in higher plasma density due to a higher degree of ionization and dissociation of the precursor (CH₄) in the plasma. It is worth noting that the average ion energy was proportional to the RF power (voltage) [30]. If the RF power was too high (e.g., 60 W), film delamination could occur due to the large ion energy. Under each power, the deposition time was adjusted according to the deposition rate to produce films of ~100 nm thickness. Figure 2b shows an example of the coating thickness profile on a glass substrate measured with the profilometer. It confirms the film thickness was ~100 nm.

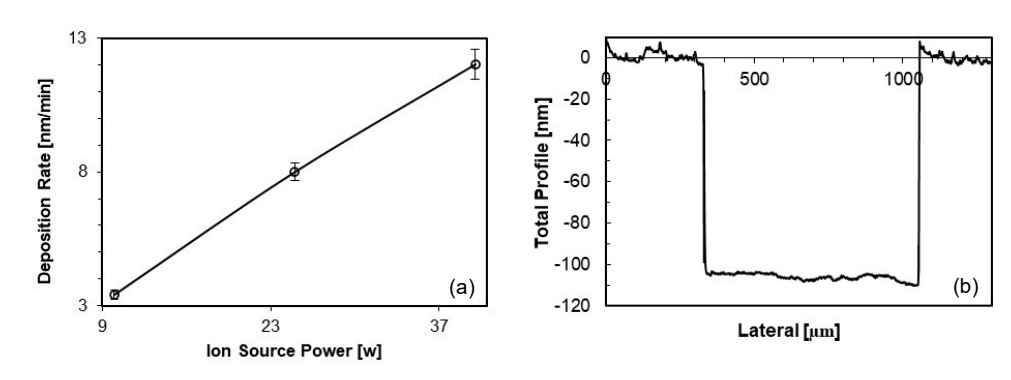


Figure 2. (a) Deposition rate dependence on the ion source RF power and (b) surface profile of the a-C:H coating on a glass substrate.

Figure 3 shows the deconvoluted XPS C 1s peak for the a-C:H film deposited at 40~W RF power as a representative of the overall structure and composition of all deposited films in this study. The curves around 283.4 and 284.6 eV can be attributed to the typical $\rm sp^2$ and $\rm sp^3$ carbon-carbon (C-C) and/or carbon-hydrogen (C-H) bonds, respectively, in a-C:H coatings. The remaining deconvoluted curves around 285.5 (C-O), 287.9 (C=O), and 289.2 eV (COOH) are due to the presence of oxygen on the film surface. Most of that oxygen is probably present because of air exposure.

Table 1 summarizes Young's modulus and film density of the a-C:H coatings. Although the film density nearly did not change, the modulus was lower at 40 W RF power compared to the other films. A decrease in Young's modulus can be an indication of hydrogen incorporation. Our recent study indicated that the average electron energy and ion energy are proportional to the RF power [30], hence, higher RF power will lead to a stronger dissociation of precursor molecules. This will raise the overall free hydrogen in the plasma, which can be incorporated into the growing film. The ratio of sp³ to sp² carbon/hydrocarbon is another main contributor to Young's modulus and density in amor-

Coatings **2022**, 12, 1159 4 of 7

phous carbon coatings. The difference in proportionality to the RF power in Young's modulus and density can be explained by those two contributors: When the RF power increases, the growing film is bombarded by ions of higher energy which appears to enhance the graphitization ($\rm sp^2$) of the deposited material. Thus, Young's modulus decreases, which can be especially observed when increasing the RF power from 25 to 40 W. This effect is not as apparent when rising the RF power from 10 to 25 W, which could indicate that the bombarding ion energies are not high enough to transform some of the $\rm sp^3$ bonds to $\rm sp^2$ bonds. The possible increase in $\rm sp^2$ carbon also decreases the overall density of the film, but the incorporation of free hydrogen on interstitial spots appears to counteract this process.

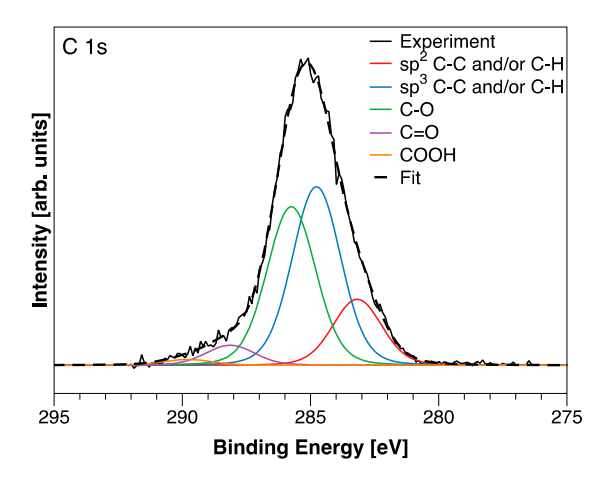


Figure 3. XPS spectrum of the a-C:H film deposited at 40 W RF power.

Table 1. Summary of mechanical properties of a-C:H coating.

Power (W)	Young's Modulus (GPa)	Density (g/cm ³)	Sq (nm)
10	76	1.92	1.2
25	75	1.91	1.1
40	70	1.90	1.1

Atomic force microscopy (AFM) was performed in an area of 2×2 μ m on the samples deposited on the polished Si substrates. Figure 4 shows the topography of the coatings deposited at different RF power. The calculated S_q values are summarized in Table 1. All the coatings exhibited similar root mean square roughness values of 1.1–1.2 nm. No direct correlation between the roughness and RF power could be found. Slight differences might be caused by the technique itself and are not significant.

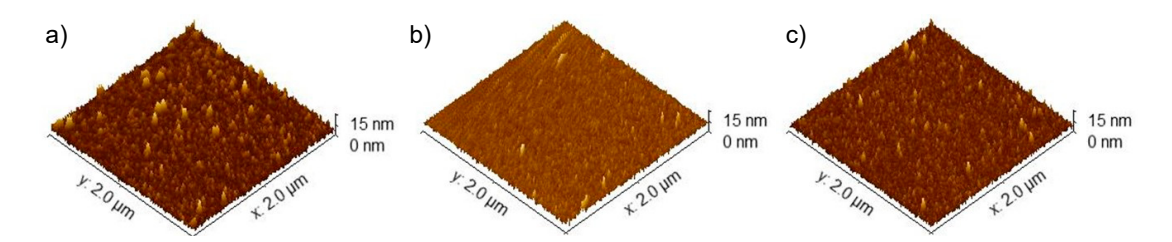


Figure 4. AFM images of a-C:H coatings on Si substrate with deposition power of (a) 10 W, (b) 25 W, and (c) 40 W.

Figure 5 shows the optical transmittance (a) and reflectance (b) spectra of the a-C:H coatings with a thickness of approximately 100 nm. The films were highly transparent, and the transmittance was over 90% in the visible light range and close to 90% even in the short wavelength range down to the absorption limit of the glass substrate (~380 nm).

Coatings **2022**, 12, 1159 5 of 7

Overall, the transmittance spectra of the coatings prepared with different RF powers were similar. There was a small increase in the transmittance around 400 nm wavelength as the deposition RF power was increased to 40 W. This result is consistent with Young's modulus data, the coatings included more hydrogen content at higher deposition power and became more transparent. The reflectance spectra of the coatings deposited at different RF powers were also similar. There is a slight increase in the reflectance in the short wavelength range as the power increases. From the transmittance and reflectance spectra, the absorption coefficients of the a-C:H coatings could be deduced.

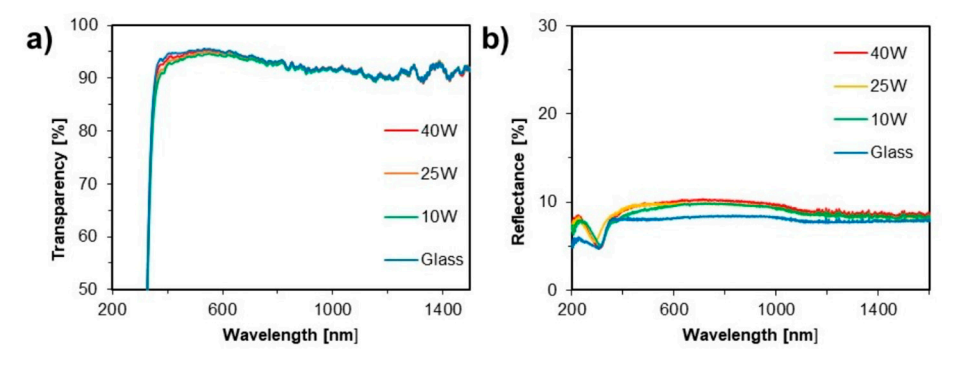


Figure 5. (a) Transmittance and (b) reflectance spectra of the a-C:H coatings produced by the ion source at different RF power.

The optical bandgap of the coatings was calculated from the transmittance (T) and reflectance (R) data, from which the absorption coefficient (α) was calculated using the following equation.

$$\alpha = \frac{1}{t} \ln \left(\frac{1 - R}{T} \right)$$

where *t* is the thickness of the coating. The optical bandgap values were estimated from the Tauc plot shown in Figure 6. The predicted optical bandgap was around 3.7 eV. The deposition power had little effect on the optical bandgap of the coatings.

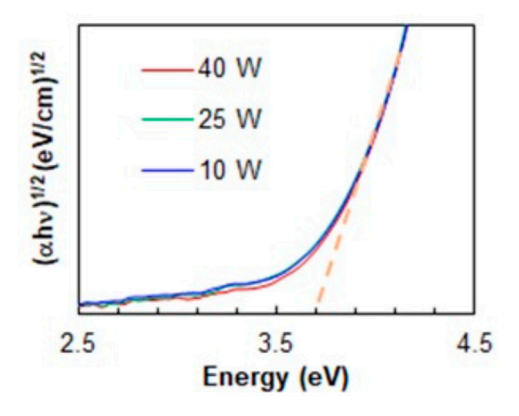


Figure 6. Tauc plot of the a-C:H coatings produced at different ion source power.

4. Conclusions

This work demonstrates the deposition of highly transparent hydrogenated amorphous carbon coatings using a single beam ion source at low temperatures. Using methane as the source gas, a-C:H coatings have a transmittance of about 90% from UV to the infrared wavelength range. The optical bandgap of the coatings is at least \sim 3.7 eV. The coatings have Young's modulus of \sim 78 GPa and a density of \sim 1.9 g/cm³ with a roughness value of \sim 1.1 nm. Higher deposition power achieved high deposition rates without decreasing the material properties significantly. The combination of high transmittance and moderate

Coatings **2022**, 12, 1159 6 of 7

Young's modulus makes the ion-source-deposited a-C:H coatings attractive for protecting soft and heat-sensitive surfaces.

Author Contributions: Depsoition experiment, writing-original draft, Y.K.; Young's modulus measurements, writing and reviewing-original draft preparation, N.B.; experiment set up and reviewing-original draft, M.S.; funding acquision, project administration, reviewing of draft and supervision, Q.H.F. All authors have read and agreed to the published version of the manuscript.

Funding: National Science Foundation awards #1917577 and #1724941. US Department of Energy award DE-EE0009018.

Institutional Review Board Statement: Not applicable.

Informed Consent Statement: Not applicable.

Data Availability Statement: Not applicable.

Acknowledgments: This work is partly supported by the National Science Foundation awards #1917577 and #1724941. Also acknowledged is the US Department of Energy award DE-EE0009018. Michigan State University Composite Materials and Structure center.

Conflicts of Interest: The authors declare no conflict of interest.

References

1. Pandey, B.; Pal, P.; Bera, S.; Ray, S.; Kar, A. Effect of nickel incorporation on microstructural and optical properties of electrode-posited diamond like carbon (DLC) thin films. *Appl. Surf. Sci.* **2012**, *261*, 789–799. [CrossRef]

- Zhou, B.; Liu, Z.; Piliptsou, D.G.; Yu, S.; Wang, Z.; Rogachev, A.V.; Rudenkov, A.S.; Balmakou, A. Structure and optical properties
 of Cu-DLC composite films deposited by cathode arc with double-excitation source. *Diam. Relat. Mater.* 2016, 69, 191–197.
 [CrossRef]
- 3. Stock, F.; Antoni, F.; Diebold, L.; Gowda, C.C.; Hajjar-Garreau, S.; Aubel, D.; Boubiche, N.E.; Le Normand, F.; Muller, D. UV laser annealing of diamond-like carbon layers obtained by pulsed laser deposition for optical and photovoltaic applications. *Appl. Surf. Sci.* 2019, 464, 562–566. [CrossRef]
- 4. Lu, Y.; Huang, G.; Wang, S.; Xi, L.; Qin, G.; Wei, J.; Chen, X. Pulsed laser deposition of the protective and Anti-reflective DLC film. *Infrared Phys. Technol.* **2021**, *119*, 103949. [CrossRef]
- 5. Lin, C.; Wei, D.; Chang, C.; Liao, W. Optical properties of diamond-like carbon films for antireflection coating by RF magnetron sputtering method. *Phys. Procedia* **2011**, *18*, 46–50. [CrossRef]
- 6. Safari, R.; Sohbatzadeh, F.; Mohsenpour, T. Optical and electrical properties of N-DLC films deposited by atmospheric pressure DBD plasma: Effect of deposition time. *Surf. Interfaces* **2020**, *21*, 100795. [CrossRef]
- 7. Písařík, P.; Jelinek, M.; Smetana, K.; Dvořánková, B.; Kocourek, T.; Zemek, J.; Chvostová, D. Study of optical properties and biocompatibility of DLC films characterized by sp3 bonds. *Appl. Phys. A* **2012**, *112*, 143–148. [CrossRef]
- 8. Seker, Z.; Ozdamar, H.; Esen, M.; Esen, R.; Kavak, H. The effect of nitrogen incorporation in DLC films deposited by ECR Microwave Plasma CVD. *Appl. Surf. Sci.* **2014**, *314*, 46–51. [CrossRef]
- 9. Ma, W.J.; Ruys, A.J.; Zreiqat, H.; Mason, R.; Ringer, S.P.; Liu, Z.W.; Keast, V.; Martin, P.J.; Bendavid, A. The biocompatibility of diamond-like carbon nano films. In Proceedings of the 2006 International Conference on Nanoscience and Nanotechnology, Basel, Switzerland, 30 July–4 August 2006.
- 10. Jiang, X.; Reichelt, K.; Stritzker, B. The Hardness and Young's modulus of a-C:H films. Vacuum 1990, 41, 1381–1382. [CrossRef]
- 11. Lin, Z.; Wang, F.; Gao, D.; Ba, D.; Liu, C.; Zeng, L.; Feng, W.; Ding, G.; Dechun, B.; Chunming, L. Frictional and optical properties of diamond-like-carbon coatings on polycarbonate. *Plasma Sci. Technol.* **2013**, *15*, 690–695. [CrossRef]
- 12. Coşkun, D.; Zerrin, T. Optical, structural and bonding properties of diamond-like amorphous carbon films deposited by DC magnetron sputtering. *Diam. Relat. Mater.* **2015**, *56*, 29–35. [CrossRef]
- 13. Deraman, K.; Sarmid, S.; Ismail, B.; Ahmad, N.; Hussin, R.; Shamsuri, W.N.W.; Yusof, M.N.M.; Hamzah, K. Optical properties of diamond-like carbon thin films deposited by DC-PECVD. *Malays. J. Fundam. Appl. Sci.* **2011**, *7*, 1–5. [CrossRef]
- 14. Reddy, K.N.; Varade, A.; Krishna, A.; Joshua, J.; Sasen, D.; Chellamalai, M.; Kumar, P.S. Double side coating of DLC on silicon by RF-PECVD for AR application. *Procedia Eng.* **2014**, *97*, 1416–1421. [CrossRef]
- 15. Srinivasan, S.; Tang, Y.; Li, Y.; Yang, Q.; Hirose, A. Ion beam deposition of DLC and nitrogen doped DLC thin films for enhanced haemocompatibility on PTFE. *Appl. Surf. Sci.* **2012**, *258*, 8094–8099. [CrossRef]
- 16. Ankit, K.; Varade, A.; Reddy, N.; Dhan, S.; Chellamalai, M.; Balashanmugam, N.; Krishna, P. Synthesis of high hardness IR optical coating using diamond-like carbon by PECVD at room temperature. *Diam. Relat. Mater.* **2017**, *78*, 39–43.
- 17. Kim, W.R.; Park, M.S.; Jung, U.C.; Kwon, A.R.; Kim, Y.W.; Chung, W.S. Effect of voltage on diamond-like carbon thin film using linear ion source. *Surf. Coat. Technol.* **2014**, 243, 15–19. [CrossRef]
- 18. Markwitz, A.; Mohr, B.; Carpeño, D.F.; Hübner, R. Ultra-smooth diamond-like carbon coatings with high elasticity deposited at low temperature by direct ion beam deposition. *Surf. Coat. Technol.* **2014**, 258, 956–962. [CrossRef]

Coatings **2022**, 12, 1159 7 of 7

19. An, X.; Wu, Z.; Liu, L.; Shao, T.; Xiao, S.; Cui, S.; Lin, H.; Fu, R.K.; Tian, X.; Chu, P.K.; et al. High-ion-energy and low-temperature deposition of diamond-like carbon (DLC) coatings with pulsed kV bias. *Surf. Coat. Technol.* **2019**, *365*, 152–157. [CrossRef]

- 20. Sheng, H.; Xiong, W.; Zheng, S.; Chen, C.; He, S.; Cheng, Q. Evaluation of the sp3/sp2 ratio of DLC films by RF-PECVD and its quantitative relationship with optical band gap. *Carbon Lett.* **2021**, *31*, 929–939. [CrossRef]
- 21. Córdoba, R.; Ibarra, A.; Mailly, D.; De Teresa, J.M.M. Vertical growth of superconducting crystalline hollow nanowires by He+focused ion beam induced deposition. *Nano Lett.* **2018**, *18*, 1379–1386. [CrossRef]
- 22. Písařík, P.; Mikšovský, J.; Remsa, J.; Zemek, J.; Tolde, Z.; Jelínek, M. Diamond-like carbon prepared by pulsed laser deposition with ion bombardment: Physical properties. *Appl. Phys. A* **2018**, 124, 85. [CrossRef]
- 23. Wang, W.; Liu, L.-F.; Yao, Y.-J.; Lu, S.-D.; Wu, X.; Zheng, T.; Liu, S.-F.; Li, Y.-J. Growth dynamics controllable deposition of homoepitaxial MgO films on the IBAD-MgO substrates. *Appl. Surf. Sci.* 2018, 435, 225–228. [CrossRef]
- 24. Roth, J.R. Industrial plasma engineering. Inst. Phys. Publ. 1995, 1, 366–367.
- 25. Wolf, B. Handbook of Ion Sources; CRC Press: Boca Raton, FL, USA, 1995.
- 26. Aisenberg, S.; Chabot, R. Ion-beam deposition of thin films of diamondlike carbon. J. Appl. Phys. 1971, 42, 2953–2958. [CrossRef]
- 27. Kaufman, H.R. Technology of ion beam sources used in sputtering. J. Vac. Sci. Technol. 1978, 15, 272–276. [CrossRef]
- 28. Kaufman, H.; Raymond, R.; Robinson, S.; Seddon, R.I. End-Hall ion source. *J. Vac. Sci. Technol. A Vac. Surf. Film.* 1987, 5, 2081–2084. [CrossRef]
- 29. Fan, Q.H.; Schuelke, T.; Haubold, L.; Petzold, M. Single Beam Plasma Source. US Patent #11049697, 29 June 2021.
- 30. Tran, T.; Kim, Y.; Baule, N.; Shrestha, M.; Zheng, B.; Wang, K.; Schuelke, T.; Fan, Q.H. Single-beam ion source enhanced growth of transparent conductive thin films. *J. Phys. D Appl. Phys.* **2022**, *55*, 395202. [CrossRef]